scientific reports

Check for updates

OPEN

Neurochemical dynamics during two hypnotic states evidenced by magnetic resonance spectroscopy

Nuno Miguel Prates de Matos[1,2], Philipp Staempfli[3], Niklaus Zoelch[1,4], Erich Seifritz[1] & Mike Bruegger[1,2]✉

This study explores neurochemical changes in the brain during hypnosis, targeting the parieto-occipital (PO) and posterior superior temporal gyrus (pSTG) regions using proton magnetic resonance spectroscopy (MRS). We examined 52 healthy, hypnosis experienced participants to investigate how two different hypnotic states of varying depth impacted brain neurochemistry in comparison to each other and to their respective non-hypnagogic control conditions. Alongside neurochemical assessments, we recorded respiration and heart rate variability (HRV) to further explore possible associations between physiological correlates of hypnotic depth. Significant changes in myo-Inositol concentration relative to total creatine were observed in the PO region during the deeper hypnosis state, possibly indicating reduced neuronal activity. No significant neurochemical shifts were detected in the pSTG region. Additionally, our findings revealed notable physiological changes during hypnosis. Respiratory rates were significantly slowed in both hypnotic states compared to the respective controls, with more pronounced slowing in the deeper hypnotic state. This study contributes a first-time insight into neurochemical responses during hypnotic states. We hope offering a foundation for further research in understanding the neurobiological correlates of hypnosis in both, basic science and—down the line—clinical applications.

Hypnosis has been defined by the American Psychological Association (APA) as "a state of consciousness involving focused attention and reduced peripheral awareness characterized by an enhanced capacity for response to suggestion."[1]. To induce these altered states, a hypnotist or hypnotherapist typically begins a hypnosis session with an induction, where they provide specific verbal instructions to a subject[2]. Research into the phenomenology of hypnotic states suggests a more complex scenario than that depicted by the APA definition. This includes a decrease in peripheral awareness, reduced judgment and monitoring, a loss of time and spatial orientation, and at times, experiences of automatic or involuntary motor responses[3–7]. The hypnotic induction without further suggestions is also frequently referred to as "neutral hypnosis"[8].

Over recent decades, extensive research has focused on the effects of neutral hypnosis on brain processes, often utilizing functional magnetic resonance imaging (fMRI). Common to the results of the studies conducted are changes in activity and connectivity in areas that are part of the default-mode (DMN), salience (SN) and central executive networks (CEN)[9–17]. Hypnosis research has attributed particular importance to these brain networks, as they have been linked to the control and monitoring of attention, regulation of sensory and interoceptive processes, which are discussed as central elements of hypnosis[4,18]. An activation likelihood estimates (ALE) meta-analysis conducted by Landry et al.[4] aimed at identifying consistent neural correlates of hypnosis and hypothesized the involvement of the CEN, SN and DMN as a commonality across the included neuroimaging studies. However, rather than confirming their hypotheses, ALE findings showed a link between hypnosis and medial lingual gyrus, an occipital area primarily commonly reported to be engaged in advanced visual processing. Although the lack of confirmation of the involvement of CEN, SN and DMN by the meta-analysis is partly attributable to the substantial heterogeneity of applied technical methodologies and hypnotic procedures in the included studies, the surprising finding could also be viewed as an invitation for the exploration of hypnosis correlates beyond DMN, SN, CEN and the concept of top-down model of hypnosis[4].

In a previous fMRI-study from our group, which was conducted in the context of "Project HypnoScience", hypnosis-related brain connectivity was explored by means of a purely data driven functional connectivity

[1]Department of Adult Psychiatry and Psychotherapy, Psychiatric University Clinic Zurich and University of Zurich, Zurich, Switzerland. [2]Clinic of Cranio-Maxillofacial and Oral Surgery, Center of Dental Medicine, University of Zurich, Zurich, Switzerland. [3]MR-Center for Child, Adolescent and Adult Psychiatric-Psychotherapeutic Research, Psychiatric University Clinic Zurich and University of Zurich, Zurich, Switzerland. [4]Institute of Forensic Medicine, University of Zurich, Zurich, Switzerland. ✉email: mike.bruegger@bli.uzh.ch

multivariate pattern analysis (fc-MVPA)[19,20]. This method analyzes the connectivity of individual voxels with the entire brain, providing a comprehensive map of functional connectivity without the necessity of a-priori limitations on areas or networks, like for example SN, DMN and CEN. Clusters identified through this method represent areas where the pattern of connectivity with the rest of the brain significantly differs, either between different conditions or across subject groups[20]. In this previous work, two hypnotic states differing in hypnotic depth (Hypnotic state 1 and 2, HS1 and HS2) were compared with matched non hypnagogic control conditions (control state 1 and 2, CS1 and CS2)[19]. Using the fc-MVPA approach, significant clusters were identified for the comparison for each of the hypnosis states with the corresponding control condition (HS1 vs CS1 and HS2 vs CS2). Interestingly, the most significant clusters identified in the comparisons HS1 vs CS1 and HS2 vs CS2, were highly similar in shape and location, encompassing parieto-occipital (PO) structures such as (pre-) cuneal cortex, intra- and supracalcarine cortex, lateral occipital cortex and bilateral lingual gyrus. The lingual gyrus emerged as part of these clusters, being the structure, which most strongly correlated in the meta-analysis performed by Landry et al.[4]. When comparing both hypnotic states with each other (HS1 vs HS2), a PO-cluster did not emerge, possibly pointing to its central connective role in both states. Instead, a temporal cluster (pSTG cluster) involving the posterior part of the left superior temporal gyrus, left supramarginal and middle temporal gyrus was identified as most significant[19]. However, while the fMRI study's identification of the PO and pSTG indicates their significant role in differentiating network configurations between hypnosis and control states, as well as between the two hypnosis states themselves, the results do not provide information about changes in neurophysiological processes inside the clusters themselves independent of their network context.

The goal of the present study focuses on the neurochemical milieu during hypnosis. As the second study in the HypnoScience-project, neurochemical alterations within these two core areas were measured, by means of proton magnetic resonance spectroscopy (MRS).

MRS has a different strength profile, with its low spatial resolution of cubic centimeters and temporal resolution of minutes[21]. The strength of this method lies in the capability to directly acquire signals on the neurochemical components within regions-of-interest, such as excitatory (glutamate, Glu) and inhibitory (γ-Aminobutyric acid, GABA) neurotransmitters, neuronal viability (*N*-Acetylaspartate, NAA), energy (creatine) and cell membrane (choline) metabolism as well as compounds involved in cellular signaling, osmoregulation and neuronal activity (myo-Inositol, mI)[22,23]. Thus, this technique has the potential to provide information about the neurochemical fingerprint of the functional PO and pSTG areas during hypnosis. To the authors knowledge, this study explores for the first time by means of MRS the neurochemical milieu in two brain regions during hypnosis. The selected two brain regions possibly play fundamental roles in regulating hypnotic states as indicated by the results of the previous fMRI study. Based on the fMRI observations, we hypothesize in the present study that (1) the functional PO area shows similar neurochemical alterations in both hypnotic states compared to the control conditions, but not between the hypnotic states themselves (main effect of hypnosis). In other words, PO shows specificity for hypnosis, but not for differences in depth of the hypnotic states. Furthermore, (2) we hypothesize that pSTG shows neurochemical alterations between hypnotic states 1 and 2.

For that purpose, 52 healthy hypnosis-experienced participants were included in the study. Neurochemical assessments were complemented by respiration, heart rate (variability) measures and questionnaire data.

Materials and methods

Subjects

The study was approved by and conducted according to the regulations of the ethics committee of the Canton of Zurich (BASEC No. 2018-00550). The research was conducted in accordance with the Declaration of Helsinki. All participants received detailed information about the experimental procedure, the aim of the study, and gave their written informed consent before any procedures were carried out. Participants were instructed not to consume alcohol, analgesics/other medications 24 h before the start of the experiment and to eat before arriving at the study site. The study was conducted at the MR centre of the Psychiatric University Hospital Zurich, Switzerland.

For this study, a total of 52 subjects (34 females, 18 males, mean age 46.9) were recruited.

The experimental procedure was identical for the fMRI and MRS study and is described in detail in the fMRI manuscript[19]. Recruitment focused on participants familiar with the hypnosis procedures used in this study. Participants underwent basic hypnosis training (Hypnose.NET GmbH/OMNI Hypnosis International). All of them practiced self-hypnosis on a weekly basis for at least two months. The rationale behind this requirement was to ensure a sufficient level of familiarity with the subjective experience to provide feedback on the perceived hypnotic states experienced within the scanner. As many of the participants were exposed to a MR-scanner for the first time, the question arose to what extent such an unfamiliar setting would impact the quality hypnotic states. The familiarity with the states allowed the participants to compare the perceived states inside the scanner with states typically perceived in their well-known environment. Comparability was assessed by means of the questionnaire.

Experimental design

The experimental design and procedure are illustrated in Fig. 1. The experiment had of a total of four conditions: Two hypnosis (Hypnotic state 1 and 2; HS1/HS2) and two corresponding control conditions (control state 1 and 2; CS1/CS2). Each condition consisted of induction and measurement phase. Participants were randomly allocated to either sequence 1 or 2 of the experimental procedure.

In the induction phase, hypnosis and control inductions were acoustically presented to the participants by experienced hypnotherapists via high-fidelity MR-headphones (MRConfon, Magdeburg, Germany) while the participants were comfortably positioned inside the scanner in a supine position. During the induction phases, no MR-measurements were done. The hypnotic inductions consisted of standardized texts based on the Dave Elman induction techniques, which were adapted to the MR scanner environment and translated to

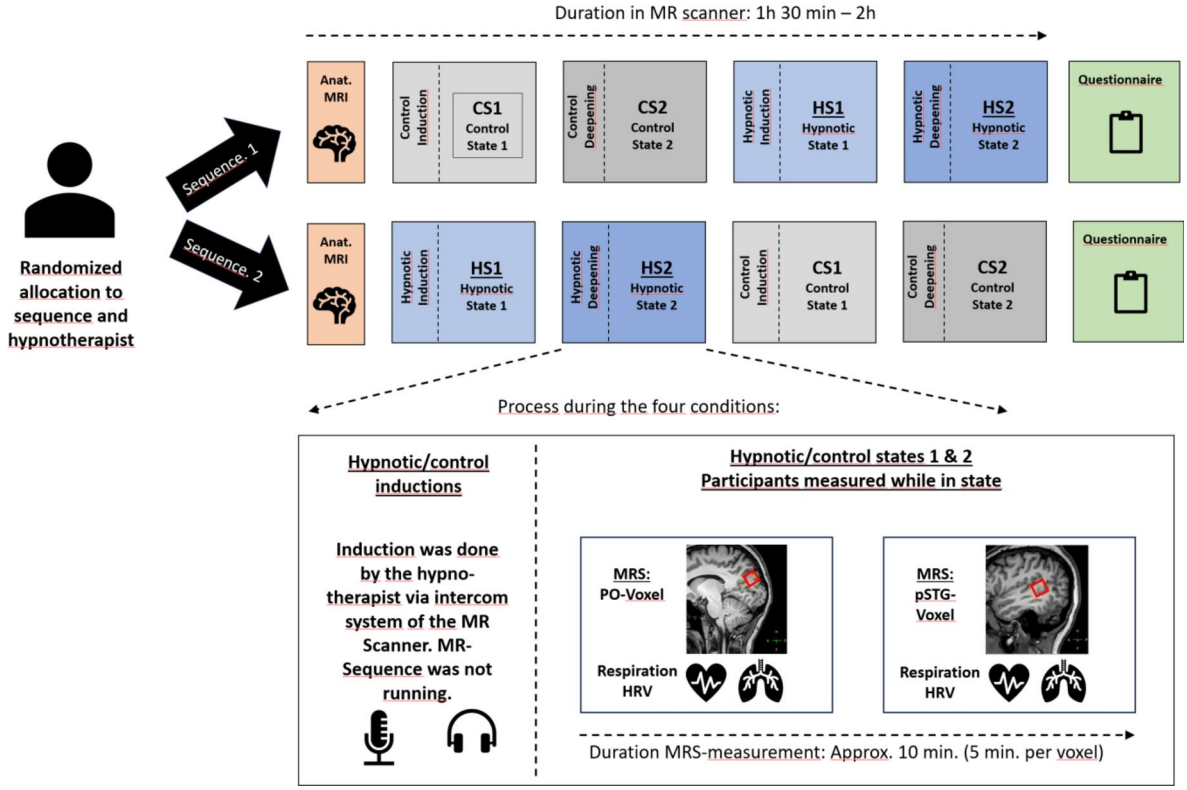

Fig. 1. Illustration of experimental setup. Participants were randomly allocated to two different experimental sequences to counterbalance sequential effects. Both sequences were identical except that for sequence 1, the control conditions (CS1, CS2) were performed first, followed by the hypnosis induction and deepening. In sequence 2, the order was reversed. During all MRS measurements, heart rate and respiration data were recorded. In both sequences, a post-MR questionnaire was given to the participants to evaluate the comparability of the states compared to when under familiar circumstances. Furthermore, the questionnaire also assessed stability of the states during the measurements, tiredness of the participants during the measurements and applied effort to maintain the states (including wakeful state during control conditions).

German (Hypnose.NET GmbH/OMNI Hypnosis International). The first hypnotic induction aimed at guiding the participants into a state of profound mental and physical relaxation (HS1), whereas the second hypnotic (deepening) induction aimed at further deepening the state into a deep state commonly characterized by a suspension of time and localization orientation and experience of automatic or extra-volitional own (motor) responses[3–7]. Control inductions were designed based on the work of Varga et al.[6] and consisted of a collage of Wikipedia snippets which were topic-related to the sections of the hypnotic inductions. For more details regarding hypnosis and control induction texts and hypnosis procedures, see Matos et al.[19].

Following the induction procedures, the MRS-measurements were started and lasted approx. 10 min per condition. During the MRS measurements, heart rate was recorded by means of a pulse oximeter (PPU) sensor and respiration data was collected via a respiratory belt (Philips Medical Systems, Best, The Netherlands).

At the end, participants completed a questionnaire consisting of four items in which the participants provided information about the quality and stability of the experienced states, the exerted effort to remain in the states and the level of perceived sleepiness.

MRI data acquisition and analysis

MR data was acquired on a Philips Achieva 3T scanner with a dStream upgrade (Philips Medical Systems, Best, The Netherlands) using a dStream 32-Channel head coil. For information regarding the fMRI sequences and applied MVPA-based connectivity analyses, see Matos et al.[19].

Anatomical MRI

A T1-weighted 3D TFE (Turbo-Field-Echo) sequence was done at the beginning of the measurement sessions. The MRS-voxel placements were done on these T1w images. The parameters were as follows: 160 sagittal slices, repetition time (TR) = 8.16 ms, echo time (TE) = 3.73 ms, acquisition voxel size = $1.0 \times 1.0 \times 1.0$ mm^3, flip angle = 8°, FOV = $240 \times 240 \times 160$ mm^3, acquisition matrix 240×240 pixels, scan duration 7 min 32 s.

MRS protocol

A standard single-voxel PRESS (point-resolved spectroscopy) sequence (TR/TE 2500/32 ms; data points = 1024; sample frequency = 2000 Hz; readout duration = 512 ms; number of acquisitions = 128) was used to obtain the

spectra. To improve spectral quality and to reduce the effects of frequency drifts, the 128 acquisitions were divided into four dynamic blocks containing 32 acquisitions each. A total of four successive PRESS sequences (4 × 32 acquisitions) per voxel were performed per block. A water-unsuppressed spectrum was acquired prior to the main spectrum for post hoc spectral corrections. Water suppression was achieved using a VAPOR (variable pulse power and optimized relaxation delays) scheme[24]. A second-order projection-based shimming routine was used for the reduction of B_0-inhomogeneities[25]. Shim volume was placed manually and asymmetrically regarding the measurement voxel to avoid the inclusion of surrounding heterogeneous tissues, thus reducing B_0-inhomogeneities.

MRS voxel definition and placements

As described in the introduction section, the MRS Voxels were positioned in the PO and pSTG regions, based on the fc-MVPA results revealed in Matos et al.[19] Specifically, the PO-voxel was defined according to the observation that the most significant and largest clusters for the contrasts HS1 vs CS1 and HS2 vs CS2 strongly overlapped (For details see Clusters 1 of both, HS1 vs CS1 and HS2 vs CS2 (Fig. 3) in[19]). We interpreted this observation as a possible role of this region in mediating states of hypnosis independent on depth. For this reason, the commonality of these fc-MVPA clusters in the fMRI-dataset was analyzed by contrasting the hypnosis vs control conditions (main effect of condition) independent of depth (Fig. 2, upper row). The strongest cluster resulting from the main effect of hypnosis did correspond to the cluster 1 of both HS1 vs CS1 and HS2 vs CS2, as expected (Fig. 2). The peak voxel of this cluster was then estimated to identify the ideal position for the MRS measures (Fig. 2) using the SPM12-toolbox (https://www.fil.ion.ucl.ac.uk/spm/software/spm12/) running on MATLAB V2018b (MathWorks, Natick, USA). The identified peak voxel MNI-coordinates were: 12 −80 36. These results were then used as orientation guideline for the manual placement of the voxels in the PO region for each study subject.

The second MRS voxel (pSTG) was defined based on the HS1 vs HS2 fc-MVPA contrast in the fMRI-study in order to focus on possible neurochemical effects linked to mediate the two depth levels of the induced hypnosis. For that purpose, the peak voxel (MNI-coordinates: −58 −42 6) of the fc-MVPA-cluster 1 of the HS1 vs HS2 contrast was estimated and, analogous to the PO-voxel, used as visual reference for the manual placement the pSTG-MRS voxel for each participant.

For both voxels, the same dimensions were chosen, namely: 18 mm × 17 mm × 17 mm (Fig. 2).

To assess the variability in voxel placement for the PO and pSTG-region between all volunteers, a voxel overlay analysis was conducted using the Osprey toolbox v2.7.0 running on MATLAB R2023a (MathWorks, Natick, USA). First, individual PO- and pSTG-voxels were coregistered to the anatomical T1-images. Next, co-registered voxels and T1-images were normalized to MNI-space to improve comparability of voxel placements. Results are shown in the bottom row of Fig. 2.

MRS-data preprocessing and neurochemical quantification

Before spectral quantification, following pre-processing steps were performed according to the consensus recommendations: (1) Eddy-current correction (2) combination of head coil channels, (3) frequency realignment of the 128 single acquisitions, (4) filtering of residual water signal[26]. LCModel was used when quantifying the preprocessed spectral data[27]. For quantification a basis set was simulated using the GAMMA Simulation package[28] with the following model spectra: N-acetylaspartate (NAA), N-acetyl-aspartyl-glutamate (NAAG), glutamate (Glu), glutamine (Gln), gamma-aminobutyric acid (GABA), glutathione (GSH), glycerophosphocholine (GPC), phosphocholine (PCh), creatine (Cre), phosphocreatine (PCr), myo-Inositol (mI), ethanolamine and phosphorylethanolamine (PE), aspartate (Asp), glucose (Glc), lactate (Lac), scyllo-inositol (sI), and taurine (Tau). The chemical shift range for the fitting procedure was set to 4.0–0.2 ppm. Peak area concentrations were corrected for the number of contributing protons and scaled to total creatine. The advantage of the use of creatine as internal reference is that reference and metabolite peaks are both present in the same spectrum. Therefore, as the reference signal was subject to the same influences as the rest of the spectrum, residual external effects like dynamic linewidth changes due to BOLD effects are taken into account[23].

Criteria for spectrum exclusion from the analysis were (1) linewidth of the NAA peak of > 10 Hz and signal-to-noise ratio (SNR) of < 15 (linewidth and SNR values from the LCModel analysis were used) in one of the four conditions (HS1, HS2, CS1, CS2). This means that if at least one of the spectra met the exclusion criterion, all four spectra were excluded. In addition, (2) data sets with differences in linewidth LW and SNR between the four conditions higher than two times of the mean intrasubject standard deviation (SD) of all subjects were excluded. The rationale for this approach is based on reported systematic quantification biases of neurochemical due to differences in spectral quality measures[29,30].

As neurochemical-related inclusion criterion, neurochemicals with a mean Cramer-Rao-Lower-Bound (CRLB) of < 20 were included in the analysis. We opted for a separate analysis of Glu instead of Glx (sum of Glu and Gln) as the correlation between both neurochemicals were well below the recommended cutoff-criterion of $r = |0.5|$ (PO: $r = 0.079$, $p = 0.437$; pSTG: $r = 0.030$, $p = 0.786$)[23].

Additional information regarding MRS methodology—spectral acquisition/analysis—is provided as supplementary file.

Psychophysiological data acquisition and analysis

As mentioned previously in the "Materials and methods" section, respiration and heart rate data were recorded during the four MRS recordings to assess potential psychophysiological effects associated with the hypnosis states (Sampling rate: 496 Hz). As the spectra acquisition of each voxel was divided into four dynamic blocks, four Scanphyslog text files were created per voxel. The eight text files (four from each voxel measurement) from

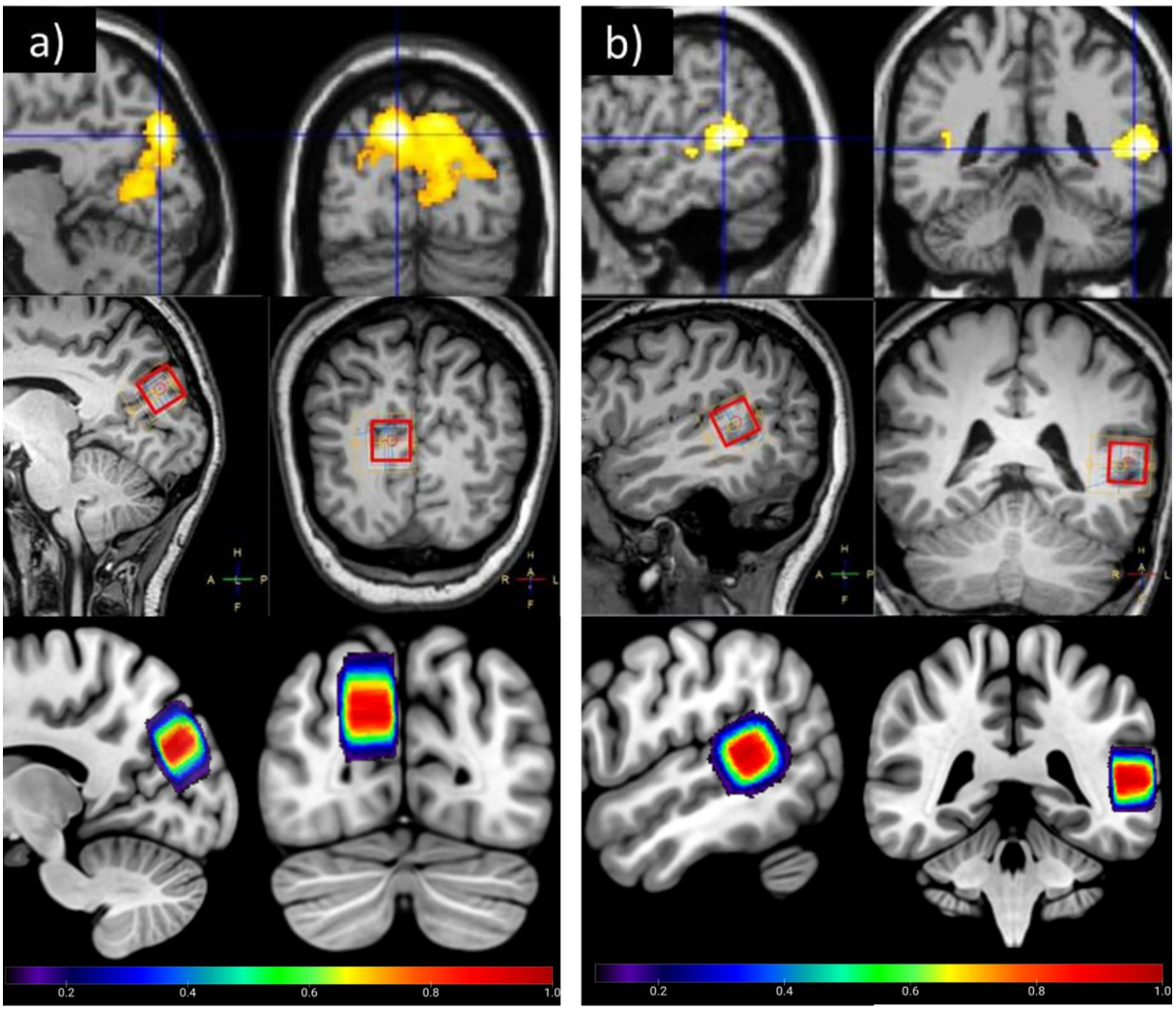

Fig. 2. Illustration of the MRS study's voxel definition and placements. Shown are six images depicting (**a**) PO and (**b**) pSTG region in sagittal and coronal orientation. The images in the top row are from the fMRI study and show the significant area (PO region) when comparing hypnotic (HS1, HS2) with control states (CS1, CS2) on group-level. The statistical thresholds set for illustrational purposes were height threshold of $p < 0.001$ (FWE) with an extended threshold $k = 10$ voxels for PO. The thresholds for the pSTG-region were height threshold of $p < 0.001$ uncorrected with extent threshold $k = 10$. The images in the middle row portray the manually positioning of the MRS voxels from a single participant based on the landmarks provided by the fMRI-study. The last row shows the voxel positioning overlaps of all participants in the MNI-space. The level of overlap is colour coded with the percent overlap indicated in the colour bar ranging from 0 (0%) to 1 (100%). Note that the illustrations are shown according to the radiological convention.

PO- and pSTG measurements were imported into LabChart Pro v8.1.2 (ADInstruments, Sydney, Australia) and appended into a single file before data analysis.

Heart rate measures

Heart rate (HR) and Heart rate variability (HRV) were calculated using the HRV module integrated in the LabChart software. This module provides automated identification of the peaks in the pulse-oximetry signal and provides HRV-estimates in the time and frequency domain. The pulse-oximetry signal was visually inspected for peak classification errors and manually corrected if necessary[31].

HR was quantified as mean beats per minute during each of the measurements. HRV was calculated as the ratio of low frequency to high-frequency (LF/HF) components in the heart rate variability signal. The LH/FH-ratio has been suggested to reflect the ratio of sympathetic (LF) to parasympathetic (HF) activity levels of the autonomous nervous system (ANS). The higher the value, the stronger the relative sympathetic activity level[32].

Respiration

First, imported respiratory signal was low-pass filtered at 0.5 Hz to remove high-frequency noise. Second, the peaks of each respiratory cycle (signalling the point of maximal inhalation) were identified using the peak

analysis toolbox included in the LabChart software package for estimation and extraction of respiratory cycle lengths. Data was visually checked for classification errors and erroneous periods were excluded.

Statistical analysis

Statistical analyses were performed using SPSS 25 (IBM Corp., Armonk, NY, USA). A statistical threshold of $p < 0.05$ was applied as significance criterion. First, the data was checked regarding normal distribution by means of a Kolmogorov–Smirnov test of normality.

Depending on distribution characteristics, the four conditions were (1) either analysed by means of an 2×2 factor analysis of variance (ANOVA) with the factors intervention (hypnosis, control) and depth (states 1 or 2), or (2) in case of non-normal distribution, were compared using a non-parametric Friedman-test. For each neurochemical and region, separate statistical analyses were performed, resulting in a total of 8 tests (two regions and four neurochemicals). Due to the study's exploratory nature, no corrections for multiple comparisons were applied at this level. In case of significances, post-hoc analyses were calculated by means of Bonferroni-corrected pairwise comparisons (four comparisons: CS1 vs CS2, HS1 vs CS1, HS2 vs CS2, HS1 vs HS2) of the estimated marginal means from the corresponding ANOVA. Bonferroni-corrected statistical thresholds of $p < 0.05$ were deemed significant (SPSS automatically adapts the Bonferroni significance level in the ANOVA post-hoc analyses to $p = 0.05$ to facilitate comparability).

Post-hoc analyses following Friedman tests were done by pairwise comparisons (four comparisons: CS1 vs CS2, HS1 vs CS1, HS2 vs CS2, HS1 vs HS2) using Wilcoxon signed-rank tests) and Bonferroni-corrected for multiple comparisons dividing $p = 0.05$ by 4, as four pairwise comparisons were calculated. Thus, the resulting Bonferroni-corrected statistical threshold was $p = 0.0125$.

Results

Analysed datasets

Regarding the MRS data, two datasets for the PO- (excess intra-subj. SD in LW) and 11 datasets for the pSTG-region (10 datasets had LW > 10 Hz, 1 dataset had SNR < 15) had to be excluded as they did not meet spectral quality requirements as specified in "Materials and methods". Thus, a total of 50 spectra for the PO and 41 for the pSTG were analyzed.

Regarding the secondary outcomes, namely the questionnaires, respiration, heart rate and heart rate variability data, the same 50 participants (evaluated in the MRS-PO analysis) were analyzed.

Questionnaire data

Descriptive statistics from the questionnaire provided by the participants to assess quality and characteristics of the different states is listed in Table 1.

Psychophysiological data

The data from the physiological parameters including mean values and corresponding standard deviations are summarized in Table 2. In addition to the mean values, alterations in respiration were summarized as percent signal changes in the supplementary material (Table S4).

HR and HRV

For heart rate, no differences between the conditions were found. However, the analysis of LF/HF ratios using a Friedman-test revealed significant differences. ($X^2 = 10.85$, $p = 0.013$). Post-hoc comparisons only found significantly higher LF/HF ratios in for the HS2 vs CS2 comparison ($Z = -3.277$, $p = 0.001$).

Respiration

The Friedman-test revealed significant differences in respiration cycle duration between the four conditions ($X^2 = 45.745$, $p = < 0.001$). Post-hoc analyses by means of Wilcoxon signed-rank tests found that respiratory cycles were significantly longer during HS1 compared to CS1 ($Z = -3.364$, $p < 0.001$). Between HS2 and CS2, the time distance between respiratory cycles was even more pronounced ($Z = -4.088$, $p < 0.001$). Regarding the comparison of both hypnosis states, mean respiration cycles were significantly longer in HS2 compared to HS1 ($Z = -2.800$, $p = 0.005$). No differences in respiration were observed when comparing CS1 and CS2.

Item	Mean (SD)			
	CS1	CS2	HS1	HS2
How comparable were the hypnotic states to those you know form OUTside the MR scanner? (1 = not at all/10 = identical)	–	–	8.55 (1.36)	8.49 (1.52)
Did the state quality change across the measurement? (1 = not at all/10 = changed completely)	2.40 (2.04)	2.38 (2.06)	2.49 (1.61)	2.76 (1.97)
Was it difficult to remain within the states? (1 = not at all/10 = very difficult)	3.65 (2.74)	3.69 (2.74)	1.83 (1.27)	1.81 (1.64)
How close were you to fall asleep? (1 = not at all/fell asleep)	2.34 (2.09)	2.25 (2.05)	1.50 (1.09)	1.37 (1.06)

Table 1. Descriptives from the hypnotic state quality questionnaire. *CS1/CS2* control states, *HS1/HS2* hypnotic states, *SD* standard deviation.

Parameter	Mean (SD)			
	CS1	CS2	HS1	HS2
Heart Rate Variability (HRV) ((Low Frequencies / High Frequencies)	1.10 (0.86)	1.19 (1.52)	1.48 (1.16)	1.58 (1.14)
Heart Rate (HR) (Beats per Minute)	65.64 (10.73)	65.64 (11.08)	65.75 (11.29)	65.56 (11.64)
Respiration (Amplitude peak-to-peak in seconds)	5.07 (1.62)	4.96 (1.68)	6.42 (3.23)	6.94 (3.69)

Table 2. Descriptives for the physiological parameters. *CS1/CS2* control states, *HS1/HS2* hypnotic states, *SD* standard deviation.

Region	Parieto-occipital (PO) Mean (SD)				Posterior superior temporal gyrus (pSTG) Mean (SD)			
Condition	CS1	CS2	HS1	HS2	CS1	CS2	HS1	HS2
Spectral quality								
$FWHM_{H20}$ [Hz]	7.45 (0.66)	7.40 (0.61)	7.36 (0.63)	7.34 (0.64)	8.26 (0.67)	8.33 (0.68)	8.2 (0.60)	8.29 (0.60)
$FWHM_{NAA}$ [Hz]	5.23 (0.83)	5.15 (0.74)	4.98 (0.74)	5.11 (0.65)	5.78 (0.82)	5.77 (0.94)	5.67 (0.76)	5.87 (0.78)
SNR_{NAA}	21.56 (2.63)	21.68 (2.67)	22.00 (3.05)	21.7 (3.12)	20.83 (3.33)	20.49 (3.07)	20.98 (3.17)	20.41 (3.18)
CRLB [%]								
tCre	2.98 (0.32)	2.94 (0.31)	2.96 (0.35)	2.86 (0.40)	2.95 (0.44)	2.98 (0.42)	2.93 (0.35)	2.98 (0.42)
Glu	6.86 (0.73)	6.74 (0.75)	6.70 (0.81)	6.86 (1.09)	6.68 (1.08)	6.90 (1.18)	6.73 (1.05)	6.78 (1.17)
tCho	5.54 (0.61)	5.5 (0.68)	5.48 (0.86)	5.38 (0.81)	4.83 (0.74)	4.98 (0.76)	4.83 (0.70)	4.90 (0.70)
tmI	5.02 (0.74)	4.94 (0.68)	4.98 (0.71)	4.88 (0.69)	4.83 (0.83)	4.95 (0.92)	4.85 (0.69)	4.85 (0.85)
tNAA	2.70 (0.46)	2.66 (0.48)	2.58 (0.50)	2.64 (0.48)	2.68 (0.47)	2.80 (0.40)	2.76 (0.43)	2.71 (0.46)

Table 3. Estimates of spectral quality and fitting errors (CRLB) of the neurochemicals included in the analysis for each condition and voxel. *CS1/CS2* control states 1 and 2, *HS1/HS2* hypnotic states 1 and 2, *SD* standard deviation, $FWHM_{H20}$ full width at half maximum of the water peak, $FWHM_{NAA}$ full width at half maximum of the NAA-peak, SNR_{NAA} Signal-to-noise ratio for the NAA-peak, *CRLB* Cramer-Rao lower bounds, *tCre* total creatine, *Glu* glutamate, *tCho* total choline, *tmI* total myo-inositol, *tNAA* total N-acetylaspartate.

MRS-data

Spectral quality

Mean spectral quality and fitting error estimates of all four states in both measured brain regions are shown in Table 3. Exemplary spectra with the spectral fits of the analyzed neurochemicals are shown in Fig. 3. Figure 4 shows an overlay of all analyzed spectra for each condition and region in order to provide an overview of the overall spectral quality. Spectral quality measures revealed good overall data quality with very low levels of intrasubject coefficient of variation (CV) between conditions. For the PO region, mean linewidth of unsuppressed water signal is 7.39 (SD = 0.62; CV = 2.4%), for pSTG 8.27 (SD = 0.63; CV = 2.2%). SNR estimates also reflect good spectra quality with mean SNR for PO of 21.92 (SD = 2.89; CV = 4.2%) and 20.68 (SD = 3.17; CV = 5.7%). This is also reflected in small fitting errors indicated by mean CRLB values of 4.56 (SD = 1.30) for PO and 4.45 (SD = 1.66) for pSTG.

Neurochemical concentrations

Table 4 presents the concentration ratios of the analysed neurochemicals using creatine as reference. Table S3 in the supplementary material summarizes neurochemical alterations between conditions as percent signal changes to provide complementary information about the effect sizes.

For PO, significant changes in tmI-concentrations were found between the four conditions as only neurochemical. The ANOVA analysis revealed a main effect of depth ($F = 5.736(1)$, $p = 0.02$, partial $\eta^2 = 0.105$) and an interaction effect of Condition (Hypnosis/Control condition) × depth ($F = 5.668(1)$, $p = 0.02$, partial $\eta^2 = 0.104$). Pairwise post-hoc comparisons found significantly higher tmI-concentrations for HS2 vs CS2 ($M_{Diff} = -0.12$, 95%-CI [0.00, 0.024], $p = 0.043$, Cohen's $dz = -0.29$) and HS2 vs HS1 ($M_{Diff} = -0.18$, 95%-CI [−0.028, −0.008], $p < 0.001$, Cohen's $dz = -0.52$) (Fig. 5).

Regarding pSTG, no significant effects were found for the reported neurochemicals.

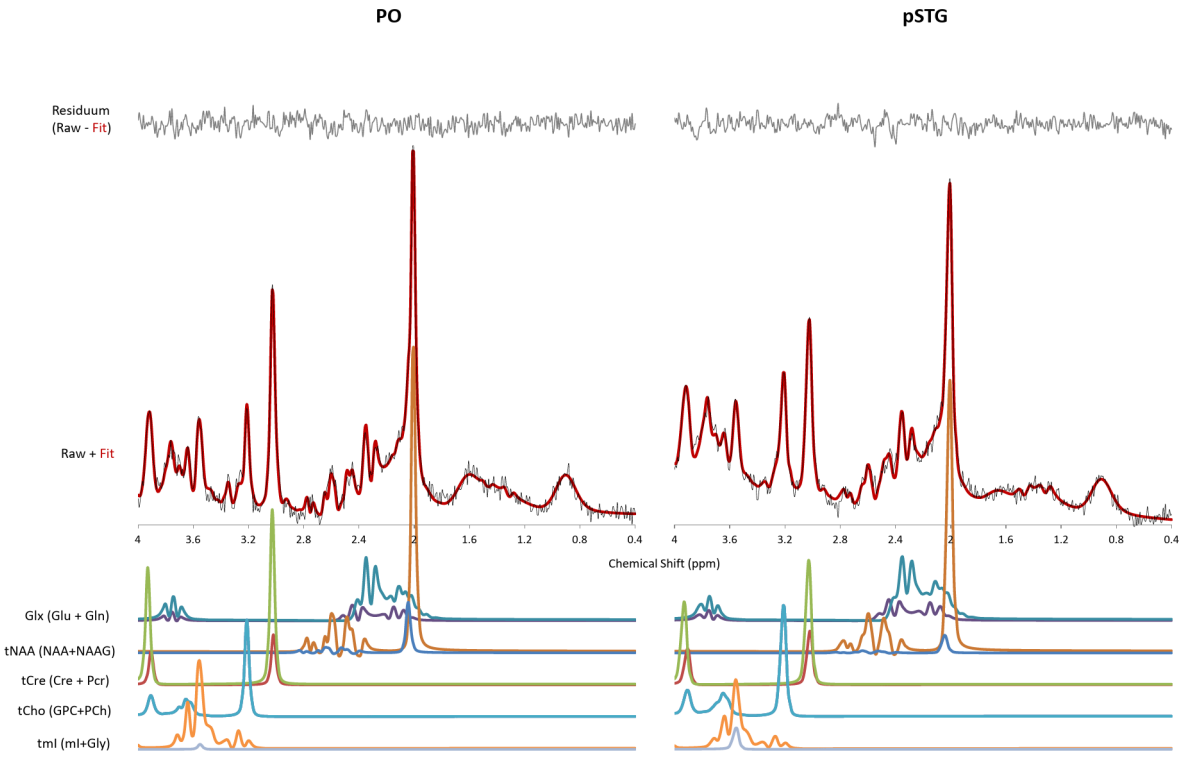

Fig. 3. Exemplary spectra from PO and pSTG fitted with LCModel. Fitted spectra (red) are superimposed with the raw spectrum (grey). Differences of fit and raw signals (residuum) are shown at the figure top. Spectra of the fitted substances are displayed below raw and fit.

Discussion

We explored neurochemical changes associated with two hypnotic states of varying depth as second investigation of a larger multimodal hypnosis project (Project HypnoScience). The present work builds on the initial fMRI related connectivity findings, applying an identical study setting with 52 hypnosis-experienced healthy participants and the same standardized hypnosis method[19]. Complementary to fMRI, we focused on alterations in the neurochemical milieu—measured via Magnetic Resonance Spectroscopy (MRS)—in two key areas identified in Matos et al.[19]. The first region (PO)—localized in the parieto-occipital junction—was defined as most strongly differentiating the hypnotic states from the control conditions, whereas the second voxel placement was defined based on most strongly differentiating both hypnotic states. This area is located within the posterior division of the left superior temporal gyrus (pSTG, see Fig. 2). Thus, we addressed the question as to whether the two hypnosis states—compared to respective control states/conditions as well as to each other—are associated with altered neurochemical profiles in the PO and pSTG voxels.

All participants were familiar with the hypnosis states, thus assessments regarding the validity of the states perceived inside the scanner was possible. Respective questionnaire data unveiled high levels of similarity inside vs outside the MR scanner with mean values of 8.55 for HS1 and and 8.49 for HS2 out of a maximum of 10 (10 corresponding to “identical”). Furthermore, questionnaire data confirmed high levels of stability and low levels of effort exerted to maintain the hypnotic and control states. Also, levels of sleepiness over the time course of the MRS measurements were low.

Note that a comprehensive neurophenomenological assessment was acquired in the EEG study of Project HypnoScience with the administration of the Phenomenology of Consciousness Questionnaire (PCI) and Altered States of Consciousness Questionnaire (ASC-11D). Due to the identical study design, study requirements and a strong overlap of participants, those results are embedded (cautiously) in the context of this study to better characterize neurochemical-behavioral associations. Questionnaire data not only uncovered evidence for HS1 and HS2 significantly differing from CS1 and CS2 in their neurophenomenological attributes, but also showed significant hypnosis depth-dependent alterations in subjective experience such as changes in emotion, attentional absorption and body perception[33].

In addition to the neurochemical and questionnaire data, respiration and heart rate data were recorded during the measurements. We found significantly slowed breathing rates in hypnosis compared to the control conditions, which is on par with the observations from the fMRI-study and with a recently published review[34]. Furthermore, we also found differences in breathing rate, with prolonged breathing cycle durations during HS2 compared to HS1. Note that slowing in respiration in HS2 compared to HS1 was also observed in Matos et al.[19], although the effect missed significancy levels (Mean respiratory cycle duration for the fMRI-study: HS1 = 6.26, HS2 = 7.17). The difference between both studies regarding this comparison is most likely attributable to the

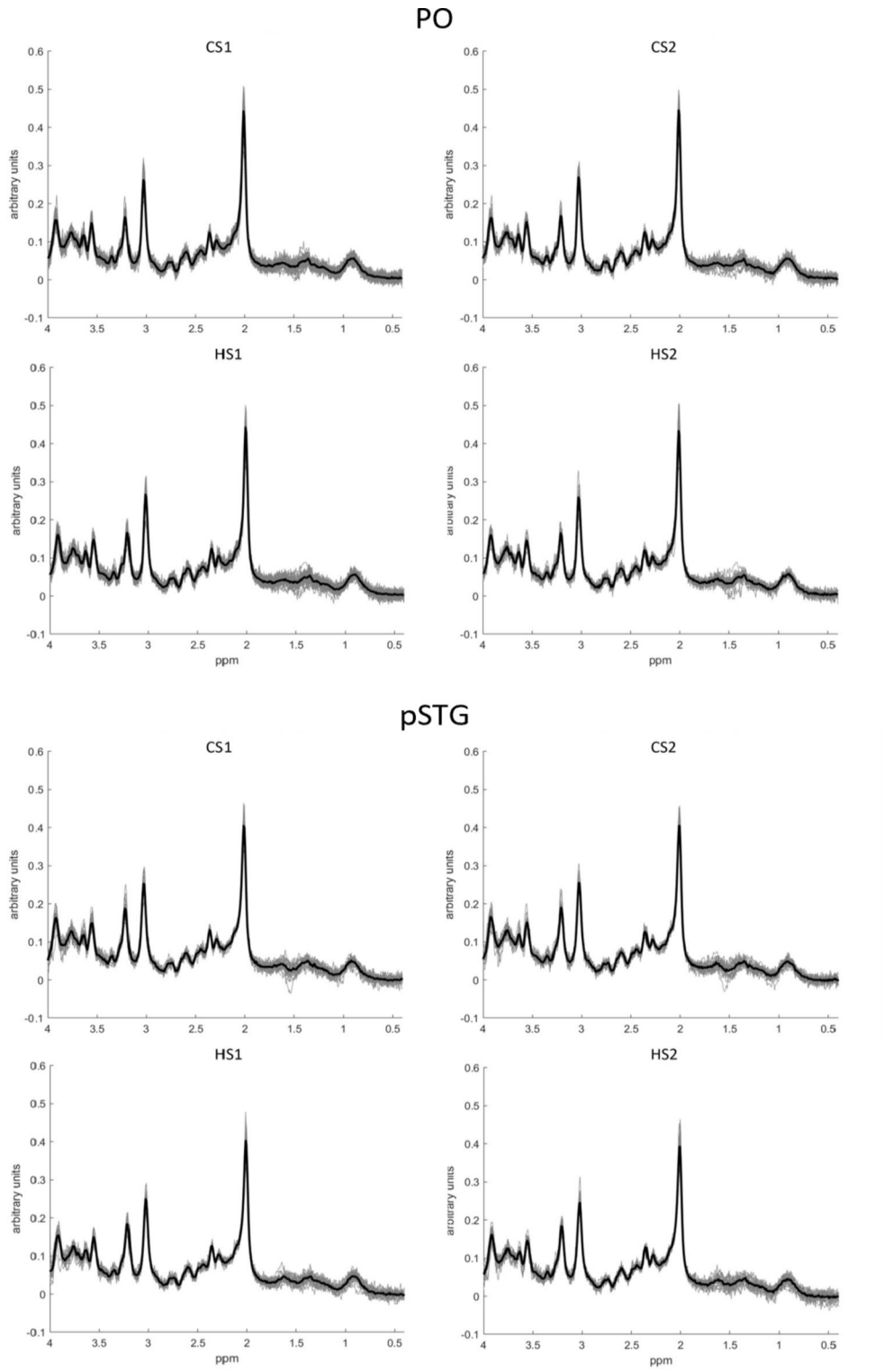

Fig. 4. Illustration of overlays of all analyzed spectra for each condition and region. All spectra are depicted in grey, the black spectra indicate the average spectra.

larger number of respiration datasets analyzed in the MRS compared to the fMRI study, thus exhibiting higher levels of statistical power.

We also observed significant alterations in heart rate variability (HRV), specifically, higher LF/HF ratios during deep hypnotic state compared to its control condition (HS2 vs CS2). However, we would like to weight these results with particular caution. The HF component of the HRV signal corresponds to the spectral power of the 0.15–0.4 Hz frequency range from the inter-beat-interval (IBI) time course[35]. The HF frequency range also

Region	Parieto occipital (PO) Mean (SD)				Posterior superior temporal gyrus (pSTG) Mean (SD)			
Condition	CS1	CS2	HS1	HS2	CS1	CS2	HS1	HS2
Neurochemicals								
Glu	1.361 (0.104)	1.366 (0.117)	1.362 (0.104)	1.347 (0.114)	1.425 (0.135)	1.403 (0.133)	1.409 (0.140)	1.410 (0.146)
tCho	0.174 (0.016)	0.176 (0.018)	0.174 (0.019)	0.175 (0.017)	0.213 (0.022)	0.212 (0.023)	0.213 (0.022)	0.212 (0.021)
tmI	0.825 (0.071)	0.825 (0.067)	0.818 (0.062)	0.837 (0.062)	0.839 (0.76)	0.833 (0.088)	0.845 (0.078)	0.840 (0.076)
tNAA	1.583 (0.114)	1.588 (0.123)	1.584 (0.111)	1.575 (0.112)	1.512 (0.119)	1.491 (0.109)	1.503 (0.101)	1.509 (0.128)

Table 4. Neurochemical concentrations (relative to creatine) for both voxels. *CS1/CS2* control states 1 and 2, *HS1/HS2* hypnotic states 1 and 2, *SD* standard deviation, *tCre* total creatine, *Glu* glutamate, *tCho* total choline, *tmI* total myo-inositol, *tNAA* total N-acetylaspartate.

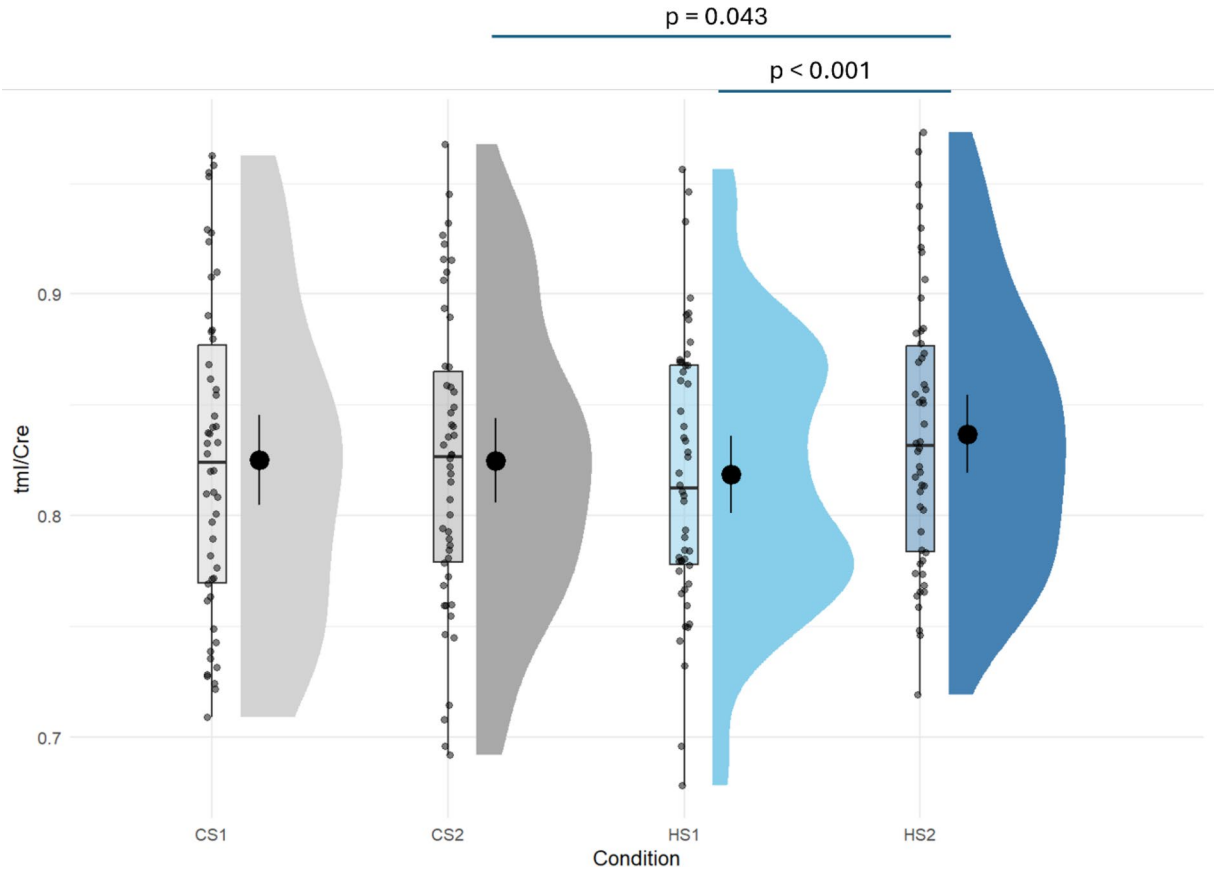

Fig. 5. Raincloud plots illustrating the tmI concentrations for the four conditions. The plots consist of a density plot for visualization of the distribution, supplemented by visualization of the mean (large dot) and 95% confidence interval (indicated by lines above and below the dot), and boxplot surrounded by scattered individual data points. Post-hoc comparisons revealed significantly higher tmI concentrations in the deeper hypnosis state (HS2) compared to its control condition (CS2) and to the less deep hypnotic state (HS1).

called the respiratory band as it reflects HR variations coupled with the respiratory cycle under the assumption that the respiratory frequency corresponds to the 0.15–0.4 Hz range[35]. However, this is not the case in the present study, as we observed mean respiration cycle durations of 6.94 for the HS2 conditions, which corresponds do frequency values of 0.14 Hz (1/6.94). Thus, the increases in the LF/HF ratios during hypnosis are most likely due to wrong attribution of the respiratory signal to the LF component (0.04–0.15 Hz), thus impede a valid interpretation of the results. For that reason, we will not discuss the HRV results further.

Neurochemical changes induced by hypnosis

The topic on neurochemical aspects of hypnosis is a novel field, with an almost inexistent body of literature. We are only aware of a conceptual work on the possible involvement on neurochemicals in hypnotic suggestions[36]

and an experimental study which explored the link between neurochemical concentrations and hypnotic suggestibility in the anterior cingulate cortex[37].

Regarding hypnotic states, the present work is—to the best of our knowledge—the first study exploring the link between hypnotic states and neurochemical alterations. Thus, the presented results must be interpreted with adequate caution and need to be regarded as preliminary until further studies have been conducted.

Due to the lack of existing work on neurochemical changes induced by hypnosis, the discussion will focus on the role of myo-inositol in neurophysiology and its role in neuroimaging work investing other modalities to create a framework for the imbedding of our finding.

Hypnosis induced changes within the Parieto-Occipital Area—PO

Regarding the PO voxel, we identified changes in the total myo-Inositol (tmI) concentrations. The ANOVA revealed a main effect of depth and interaction effect of condition (Hypnosis/Control condition) × depth, both corresponding to medium sized effects. The post-hoc comparisons identified significant differences for the comparisons HS2 vs CS2 and HS2 vs HS1 as drivers of the observed ANOVA results.

The tmI-signal reflects the sum consisting of the spectra of myo-inositol (mI) and Glycine (Gly). At field strengths of 3T, mI and Gly resonances are usually fitted as combined spectrum due to the strongly overlapping patterns (illustrated in Fig. 3). That said, in this study it is not possible to disentangle the distinct contributions from mI and Gly to the observed signal drop in tmI.

With regard to Gly, its most prominent role of Gly is its function as an inhibitory neurotransmitter and co-agonist of glutamatergic N-methyl-D-aspartate (NMDA) receptors[38]. Gly is synthetized in higher concentrations in the spinal cord and brainstem and to a lesser extent in neocortex regions[39,40].

Investigations on visual processing point towards an involvement of Gly in the visual cortex during visual stimulation in areas comparable to our PO-voxel[41,42]. Lin et al.[41] examined neurochemical dynamics in the parieto-occipital compartment of the brain using MRS at 7T. Neurochemical changes were induced using visual stimuli. They observed no effect in mI, but significant concentration reduction in Gly as response to visual stimuli. They interpreted the findings as evidence for strong neuronal activity, as Gly is a precursor for glutathione, a prominent antioxidant in the brain. Hence, the increase in glutathione synthesis during neuronal activity may result in a reduction in Gly[41]. Altered processes in areas linked to visual processing have been suggested to play a role in the HS2-state and altered states induced by psychoactive substances such as psilocybin and Lysergic acid diethylamide (LSD)[43]. Based on these observations, it is possible that the observed alterations in tmI in the HS2 state reflect increases in Gly, possibly due to hypnosis-induced changed in such parieto-occipital areas. However, the confirmation of this hypothesis necessitates a series of future studies with corresponding specific settings.

With regard to Myo-inositol, is one of the nine stereoisomer forms of the simple C_6 sugar alcohol, which together make up the inositol group. It is mainly an intracellular molecule with an overall bias towards higher concentrations in glia cells relative to neurons, substantiating its common application as a marker for glial proliferation in clinical settings[23]. This neurochemical compound usually receives less attention in functional studies, probably due to its lesser understood role in the context of neuronal activity.

There is some research showing mI alterations in processing other modalities in both, animals and humans (but no hypnosis intervention). For example, an animal study observed an acute reduction of approx. 4% in mI in the contralateral somatosensory cortex during electrical forepaw stimulation in anaesthetized rats[44]. In the same vein, Gutzeit et al. performed a series of experiments which measured neurochemical reactions to an experimental dental pain stimulus in the human insular cortex. In their first study, a reduction of 9.7% were observed in the left insula during pain stimulation[45]. In a follow-up study, Gutzeit et al. observed again a reduction (mean reduction of 6.97% compared to baseline over all areas) in mI during pain stimulation in sub-areas of the insular cortex[46]. Previous work from the same group investigating fMRI-correlates of acute dental pain using the same experimental dental pain model found an increase in the BOLD-contrast during pain in the same areas of the insular cortex[47,48]. Therefore, it could be assumed that the drop in mI goes along with an increase in excitatory neuronal activity, which also was proposed by Xu et al.[44].

As possible driver behind alterations in mI in such functional MRS studies, the role of mI as a precursor in intracellular second messenger cycle has been discussed[23,49]. Myo-Inositol plays a central role in the phosphoinositol (PI) cycle, in which the inositol-based signaling molecule IP_3 is synthetized. IP_3 is part of the intracellular signaling cascades which evokes the release of Ca^{2+} from the endoplasmic reticulum inter alia enabling long-lasting synaptic modulations such as glutamate-dependent long-term potentiation (LTP)[50]. However, the percentage of intracellular mI involved in the PI cycle is relatively low[23], thus limiting the probability of this hypothesis as possible origin of the observed effects.

An alternative explanation may be the influence of neuronal activity related metabolic effects on mI uptake by glia and neurons, such as pH-levels, lactate concentration and extracellular acidification[23]. Neuronal activation in the human visual cortex has been linked to local acidification as shown by increases in lactate concentrations[51] and reduced pH-levels[52]. Evidence suggests that alterations in acidification has the potential to widely affect neurophysiology[53–56]. The hydrogen-myo-inositol symporter HMIT plays a major role in the uptake of mI by astrocytes and neurons. Interestingly, HMIT activity has been shown to act in a pH-dependent manner, exhibiting increased activity with higher levels of extracellular acidification[57]. In that vein, extracellular decreases in pH due to heightened levels of neuronal activity could result in increased mI-reuptake by astrocytes and neurons, allowing the mI to be metabolized. Such a process could manifest in a reduction of the mI-signal in a MRS spectrum. Based on such a perspective, it is conceivable that a reduction in overall neuronal activity could result in an increased level of mI, as observed by our study. However, to date this hypothesis remains speculative and dedicated research is needed to further validate such assumptions.

As mentioned at the beginning, the neurochemical effects induced by hypnosis are, of course, quite different from pain and visual processing. We are also aware that hypnosis-induced neurochemical response cascades are much more complex than those we observed here by means of the change in mI.

It is also important to reflect possible systematic confounders as origin of the observed changes in tmI. As mentioned before, we also found changes in respiration associated with hypnotic states. Respiration has been shown to induce perturbations in the static magnetic field (B_0) and negatively impact spectrum quality[26], thus this possibility needs to be thoroughly explored. In the present study, pre-processing of the spectra such as frequency realignment of the 128 single acquisitions and phase shift corrections were performed to correct for such physiological perturbations. As a result, differences in spectral quality are negligible as shown in Fig. 4. Furthermore, correlation analyses were performed to explore possible associations between tmI and respiratory rate. Pearson correlation analyses for the changes in respiration and tmI between HS2 and CS2 revealed no significant correlation ($r = 0.085$, $p = 0.556$). The same was done for differences between HS2 and HS1 and also revealed no significant correlation effect ($r = 0.00036$, $p = 0.998$). Therefore, we regard respiration-induced artifacts in the MRS as driver behind the observed tmI effects as highly unlikely.

As a first conclusion, studies investigating Gly and mI point towards a negative correlation of neuronal activity and concentrations of both substances. Thus, we put forward the cautious hypothesis that the observed significant increase in tmI may reflect a tonic reduction in neuronal activity in the PO region while subjects are in the deeper hypnotic state (HS2) compared to the corresponding control condition (CS2) and the less deep hypnotic state (HS1). Importantly, the observed effects between HS2 and CS2 are small with mean percent changes of 1.6%, which necessitates a cautious interpretation, particularly in combination with the increased probability of Type-I errors due to the exploratory approach. Importantly, these results need to be replicated and validated, ideally by combining MRS measurements at magnetic field strengths of at least 7 Tesla with resting-state fMRI measurements in the same setting.

Posterior superior temporal gyrus—pSTG

In contrast to the PO-region, no statistically significant changes in neurochemical concentrations were identified.

A possible reason could be rooted in the spectral quality acquired from the pSTG-region. Although the overall spectral quality of the included pSTG datasets were of good quality, their SNR and LW estimates were not as good as for the PO-region. The slightly broader linewidth and lower SNR levels could have been enough to induce sufficient levels of variance to over-mask hypnosis evoked neurochemical effects. Further on, the proximity of the voxel to the skull could have negatively impacted shimming performance, thus resulting in reduced spectral quality[23,58]. Furthermore, a total of 41 pSTG datasets were analyzed in comparison to the 50 included datasets in the PO analysis. The reduced number of included datasets could thus have impacted statistical sensitivity.

However, also reasons non-related to the spectral quality and statistical power could be taken into account. The pSTG-region was shown to be strongly involved from a functional connectivity perspective, as indicated by the fMRI findings in[19]. Although the pSTG-region was defined based on a fMRI-based functional connectivity analysis, it does not mean that the hypnotic states HS2 and HS1 are distinguishable by means of MRS as both methods (fMRI and MRS) are based on neurophysiological signals with different temporal dynamics. The MRS method creates a single average concentration estimates over the timecourse of the data acquisition and thus represents a neurochemical snapshot. Thus, overall tonic changes in neurochemical concentrations are needed between conditions for an adequate detection, and the results suggest that such tonic differences could have been observed for the PO- but not for the pSTG-region.

The performed MVPA-analysis using fMRI also creates a connectivity "snapshot" of connectivity pattern differences between HS2 and HS1. However, the signal basis of the functional connectivity analyses were BOLD-signal fluctuations in the frequency range between 0.01 and 0.1 Hz and is thus very different with regard to its temporal dynamics compared to the MRS measurements.

Please note, that this interpretation should be currently treated with caution as this study reflects the first approach measuring directly the neurochemical milieu while subjects are in hypnosis. Future research with dedicated and improved MRS-methodology as well as optimally suited MRS compatible hypnosis paradigms are needed to fully resolve this question.

Furthermore, several other regions need to be neurochemically investigated, because—as clearly shown in[19]—it is a far-reaching network of different brain areas involved in mediating hypnosis.

Limitations

First, familiarity of the study population with the hypnotic states was a prerequisite for enrollment in the study. Although this requirement allowed the comparison of the perceived states inside to outside the MR scanner, a certain confirmation bias cannot be excluded. Thus, it would be of significant importance to investigate a hypnosis-naïve population. In addition, self-reports by means of questionnaires were used for the assessment of the quality of the hypnotic states. Self-reports are prone to biases and are thus a limitation. Further research would profit from additional objective markers for the characterization of such states.

Second, the study was conducted at a field strength of 3 Tesla which is insufficient to independently resolve mI and Gly spectra. Thus, an option would be to replicate this approach at field strengths equal or higher 7 Tesla to enable an improved individual concentration estimates of mI and Gly.

Third, a single anatomical scan was acquired at the beginning of the experiment and voxel placements were done based on this image. Thus, potential shifts in voxel placements due to head motion cannot be estimated which represents a limitation. The use of a single image in the beginning was to keep the time between the hypnotic inductions (and control inductions) and neurochemical quantifications as short as possible. Future studies should include novel motion tracking techniques to enable prospective motion correction or at least the reporting of possible head movements between conditions.

In addition, we investigated two regions using MRS based on the results from our previous fMRI study[19]. In our opinion it is entirely possible that neurochemical shifts linked to hypnotic states are more pronounced reflected in other brain regions. Future studies are required to delve deeper into this topic.

Another limitation of the study concerns the exploratory statistical approach. Due to lack of MRS studies in the field of hypnosis research, we opted for an exploratory approach in order to identify potential effects in the broad neurochemical milieu and generate hypotheses for future confirmatory studies. This approach resulted in eight independent statistical analyses (four neurochemicals and two regions) for which we decided not to apply corrections for multiple comparisons as they may have substantially reduced statistical power and may have obscured potentially meaningful findings in this quite novel area of research. We thus followed the approach of transparency, reporting all of the conducted analyses. As a consequence, this approach inflated the probability for Type-I errors, which demands the interpretation of the reported results with a grain of salt and the necessary caution. The reported findings and proposed hypotheses need to be replicated in future studies by means of dedicated study designs with more rigorous correction methods and larger sample sizes.

Last, although neurophenomenological assessments during the EEG-study[33] provide insights about the phenomenological landscape of the hypnotic states, a direct reference to this study is not ideal. Future studies need synchronous neurophenomenological assessments in the same setting for optimal interpretability.

Conclusions and outlook

To our knowledge, this is the first study investigating the association between neurochemical concentrations and experimentally induced hypnosis states. Thus, it is crucial to emphasize that the results must be interpreted with the scientifically correct caution. We—reluctantly—interpret the outcomes as an encouraging first contribution to understand the neural effects of hypnosis induced changes within the neurochemical milieu.

The novelty of the presented approach limits the comparability to other studies. However, an overview of non-hypnosis based MRS studies suggest a link of both—mI and Gly—to levels of neuronal activity. Relating these findings to our work suggests a potential tonic reduction in parieto-occipital neuronal activity in the HS2 state. It is also important to mention, that the results do not suggest that altered tmI levels is a hypnosis specific neurochemical reaction. Brain function in general involves a myriad of altered neurochemical compounds still to uncover in future (hypnosis related) examinations.

The lack of significant findings on neurochemical effects in the pSTG-region does not invalidate the findings in[19], as fMRI and MRS represent two methods measuring different aspects of brain function on a disparate timeline. As mentioned, MRS represents very slow and tonic effects as concentration estimates represent an average over the whole measurement (approx. 5 min per area). The signal underlying the applied functional connectivity measurements using fMRI are different with signal frequencies ranging from 0.01–0.1 Hz and thus reflect fundamentally different aspects of neurophysiology.

Future research on hypnosis evoked effects in the human neurochemical milieu need to include a larger number of regions-of-interest to better explore the underlying (neurochemical) patterns linked to these altered states of consciousness. In this vein, modern magnetic resonance spectroscopy imaging techniques (MRSI) could be applied in order to simultaneously investigate multiple brain sections[59,60]. Other non-invasive techniques for whole-head examination of single neurochemicals with the spatial resolution of fMRI are being developed and applied. This methods are based on the chemical exchange saturation transfer (CEST) effect and are particularly used to measure glutamate[61], but adaptations for imaging mI are under development[62].

Data availability

The datasets used and/or analysed during the current study are available from the corresponding author on reasonable request.

Received: 21 June 2024; Accepted: 21 November 2024
Published online: 02 December 2024

References

1. Elkins, G. R., Barabasz, A. F., Council, J. R. & Spiegel, D. Advancing research and practice: the revised APA division 30 definition of hypnosis. *Int. J. Clin. Exp. Hypnosis* **63**(1), 1–9. https://doi.org/10.1080/00207144.2014.961870 (2015).
2. Terhune, D. B. & Cardeña, E. Nuances and uncertainties regarding hypnotic inductions: toward a theoretically informed praxis. *Am. J. Clin. Hypnosis* **59**(2), 155–174. https://doi.org/10.1080/00029157.2016.1201454 (2016).
3. Bicego, A., Rousseaux, F., Faymonville, M.-E., Nyssen, A.-S. & Vanhaudenhuyse, A. Neurophysiology of hypnosis in chronic pain: A review of recent literature. *Am. J. Clin. Hypnosis* **64**(1), 62–80. https://doi.org/10.1080/00029157.2020.1869517 (2022).
4. Landry, M., Lifshitz, M. & Raz, A. Brain correlates of hypnosis: A systematic review and meta-analytic exploration. *Neurosci. Biobehav. Rev.* **81**, 75–98. https://doi.org/10.1016/j.neubiorev.2017.02.020 (2017).
5. Price, D. D. & Barrell, J. J. *Inner Experience and Neuroscience* (The MIT Press, 2012).
6. Varga, K., Kekecs, Z., Myhre, P. S. & Józsa, E. A neutral control condition for hypnosis experiments: "Wiki" text. *Int. J. Clin. Exp. Hypnosis* **65**(4), 429–451. https://doi.org/10.1080/00207144.2017.1348833 (2017).
7. Zahedi, A. & Sommer, W. How hypnotic suggestions work-critical review of prominent theories and a novel synthesis (2021).
8. Kihlstrom, J. F. & Edmonston, W. E. Alterations in consciousness in neutral hypnosis: distortions in semantic space. *Am. J. Clin. Hypnosis* **13**(4), 243–248. https://doi.org/10.1080/00029157.1971.10402120 (1971).
9. Deeley, Q. et al. Modulating the default mode network using hypnosis. *Int. J. Clin. Exp. Hypnosis* **60**(2), 206–228. https://doi.org/10.1080/00207144.2012.648070 (2012).
10. Demertzi, A. et al. Hypnotic modulation of resting state fMRI default mode and extrinsic network connectivity. *Prog. Brain Res.* **193**, 309–322. https://doi.org/10.1016/B978-0-444-53839-0.00020-X (2011).
11. Jiang, H., White, M. P., Greicius, M. D., Waelde, L. C. & Spiegel, D. Brain activity and functional connectivity associated with hypnosis. *Cereb. Cortex (New York, N.Y.: 1991)* **27**(8), 4083–4093. https://doi.org/10.1093/cercor/bhw220 (2017).

12. Lipari, S. et al. Altered and asymmetric default mode network activity in a "hypnotic virtuoso": an fMRI and EEG study. *Conscious. Cogn.* **21**(1), 393–400. https://doi.org/10.1016/j.concog.2011.11.006 (2012).
13. McGeown, W. J., Mazzoni, G., Venneri, A. & Kirsch, I. Hypnotic induction decreases anterior default mode activity. *Conscious. Cogn.* **18**(4), 848–855. https://doi.org/10.1016/j.concog.2009.09.001 (2009).
14. McGeown, W. J., Mazzoni, G., Vannucci, M. & Venneri, A. Structural and functional correlates of hypnotic depth and suggestibility. *Psychiatry Res.* **231**(2), 151–159. https://doi.org/10.1016/j.pscychresns.2014.11.015 (2015).
15. Rainville, P. et al. Cerebral mechanisms of hypnotic induction and suggestion. *J. Cogn. Neurosci.* **11**(1), 110–125. https://doi.org/10.1162/089892999563175 (1999).
16. Rainville, P., Carrier, B., Hofbauer, R. K., Bushnell, C. M. & Duncan, G. H. Dissociation of sensory and affective dimensions of pain using hypnotic modulation. *Pain* **82**(2), 159–171. https://doi.org/10.1016/S0304-3959(99)00048-2 (1999).
17. Rainville, P., Hofbauer, R. K., Bushnell, M. C., Duncan, G. H. & Price, D. D. Hypnosis modulates activity in brain structures involved in the regulation of consciousness. *J. Cogn. Neurosci.* **14**(6), 887–901. https://doi.org/10.1162/089892902760191117 (2002).
18. Landry, M. & Raz, A. Hypnosis and imaging of the living human brain. *Am. J. Clin. Hypnosis* **57**(3), 285–313. https://doi.org/10.1080/00029157.2014.978496 (2015).
19. de Matos, N. M. P., Staempfli, P., Seifritz, E., Preller, K. & Bruegger, M. Investigating functional brain connectivity patterns associated with two hypnotic states. *Front. Hum. Neurosci.* **17**, 1286336. https://doi.org/10.3389/fnhum.2023.1286336 (2023).
20. Nieto-Castanon, A. Brain-wide connectome inferences using functional connectivity MultiVariate Pattern Analyses (fc-MVPA). *PLoS Comput. Biol.* **18**(11). https://doi.org/10.1371/journal.pcbi.1010634 (2022).
21. Stagg, C. & Rothman, D. L. *Magnetic Resonance Spectroscopy. Tools for Neuroscience Research and Emerging Clinical Applications* (Academic Press, 2013).
22. de Matos, N. M. P., Hock, A., Wyss, M., Ettlin, D. A. & Brügger, M. Neurochemical dynamics of acute orofacial pain in the human trigeminal brainstem nuclear complex. *NeuroImage* **162**, 162–172. https://doi.org/10.1016/j.neuroimage.2017.08.078 (2017).
23. Stagg, C. J. & Rothman, D. L. *Magnetic Resonance Spectroscopy. Tools for Neuroscience Research and Emerging Clinical Applications* (Elsevier/Academic Press, 2014).
24. Tkáč, I. et al. Water and lipid suppression techniques for advanced 1 H MRS and MRSI of the human brain: Experts' consensus recommendations. *NMR Biomed.* **34**(5), e4459. https://doi.org/10.1002/nbm.4459 (2021).
25. Gruetter, R. Automatic, localized in vivo adjustment of all first- and second-order shim coils. *Magn. Reson. Med.* **29**(6), 804–811. https://doi.org/10.1002/mrm.1910290613 (1993).
26. Near, J. et al. Preprocessing, analysis and quantification in single-voxel magnetic resonance spectroscopy: experts' consensus recommendations. *NMR Biomed.* **34**(5), e4257. https://doi.org/10.1002/nbm.4257 (2021).
27. Provencher, S. W. Estimation of metabolite concentrations from localized in vivo proton NMR spectra. *Magn. Reson. Med.* **30**(6), 672–679. https://doi.org/10.1002/mrm.1910300604 (1993).
28. Smith, S. A., Levante, T. O., Meier, B. H. & Ernst, R. R. Computer simulations in magnetic resonance. An object-oriented programming approach. *J. Magn. Reson. Ser. A* **106**(1), 75–105. https://doi.org/10.1006/jmra.1994.1008 (1994).
29. Bartha, R. Effect of signal-to-noise ratio and spectral linewidth on metabolite quantification at 4 T. *NMR Biomed.* **20**(5), 512–521. https://doi.org/10.1002/nbm.1122 (2007).
30. de Matos, N. M. P. et al. Reproducibility of neurochemical profile quantification in pregenual cingulate, anterior midcingulate, and bilateral posterior insular subdivisions measured at 3 Tesla. *Front. Hum. Neurosci.* **10**, 300. https://doi.org/10.3389/fnhum.2016.00300 (2016).
31. de Matos, N. M. P. et al. Evaluating the effects of acupuncture using a dental pain model in healthy subjects—a randomized, cross-over trial. *J. Pain* **21**(3–4), 440–454. https://doi.org/10.1016/j.jpain.2019.08.013 (2020).
32. Cacioppo, J. T., Tassinary, L. G. & Berntson, G. *Handbook of Psychophysiology* (Cambridge University Press, 2012).
33. Niedernhuber, M. et al. An interhemispheric frontoparietal network supports hypnotic states. *Cortex* https://doi.org/10.1016/j.cortex.2024.05.008 (2024).
34. Fernandez, A., Urwicz, L., Vuilleumier, P. & Berna, C. Impact of hypnosis on psychophysiological measures: A scoping literature review. *Am. J. Clin. Hypnosis* **64**(1), 36–52. https://doi.org/10.1080/00029157.2021.1873099 (2022).
35. Shaffer, F. & Ginsberg, J. P. An overview of heart rate variability metrics and norms. *Front. Public Health* **5**, 258. https://doi.org/10.3389/fpubh.2017.00258 (2017).
36. Acunzo, D. J., Oakley, D. A. & Terhune, D. B. The neurochemistry of hypnotic suggestion. *Am. J. Clin. Hypn.* **63**(4), 355–371. https://doi.org/10.1080/00029157.2020.1865869 (2021).
37. DeSouza, D. D., Stimpson, K. H., Baltusis, L., Sacchet, M. D., Gu, M., Hurd, R. et al. Association between anterior cingulate neurochemical concentration and individual differences in hypnotizability. *Cereb. Cortex (New York, N.Y.: 1991)* **30**(6), 3644–3654. https://doi.org/10.1093/cercor/bhz332 (2020).
38. Legendre, P. The glycinergic inhibitory synapse. *Cell. Mol. Life Sci.* **58**(5–6), 760–793. https://doi.org/10.1007/pl00000899 (2001).
39. Choi, C. et al. Measurement of glycine in the human brain in vivo by 1H-MRS at 3 T: application in brain tumors. *Magn. Reson. Med.* **66**(3), 609–618. https://doi.org/10.1002/mrm.22857 (2011).
40. Probst, A., Cortés, R. & Palacios, J. M. The distribution of glycine receptors in the human brain. A light microscopic autoradiographic study using [3H]strychnine. *Neuroscience* **17**(1), 11–35. https://doi.org/10.1016/0306-4522(86)90222-8 (1986).
41. Lin, Y., Stephenson, M. C., Xin, L., Napolitano, A. & Morris, P. G. Investigating the metabolic changes due to visual stimulation using functional proton magnetic resonance spectroscopy at 7 T. *J. Cereb. Blood Flow Metab.* **32**(8), 1484–1495. https://doi.org/10.1038/jcbfm.2012.33 (2012).
42. Schaller, B., Mekle, R., Xin, L., Kunz, N. & Gruetter, R. Net increase of lactate and glutamate concentration in activated human visual cortex detected with magnetic resonance spectroscopy at 7 tesla. *J. Neurosci. Res.* **91**(8), 1076–1083. https://doi.org/10.1002/jnr.23194 (2013).
43. Moujaes, F., Rieser, N. M., Phillips, C., de Matos, N. M. P., Brügger, M., Dürler, P. et al. Comparing neural correlates of consciousness: from psychedelics to hypnosis and meditation. *Biol. Psychiatry Cogn. Neurosci. Neuroimaging*. https://doi.org/10.1016/j.bpsc.2023.07.003 (2023).
44. Xu, S., Yang, J., Li, C. Q., Zhu, W. & Shen, J. Metabolic alterations in focally activated primary somatosensory cortex of alpha-chloralose-anesthetized rats measured by 1H MRS at 11.7 T. *NeuroImage* **28**(2), 401–409. https://doi.org/10.1016/j.neuroimage.2005.06.016 (2005).
45. Gutzeit, A., Meier, D., Meier, M. L., von Weymarn, C., Ettlin, D. A., Graf, N. et al. Insula-specific responses induced by dental pain. A proton magnetic resonance spectroscopy study. *Eur. Radiol.* **21**(4), 807–815. https://doi.org/10.1007/s00330-010-1971-8 (2011).
46. Gutzeit, A. et al. Differential NMR spectroscopy reactions of anterior/posterior and right/left insular subdivisions due to acute dental pain. *Eur. Radiol.* **23**(2), 450–460. https://doi.org/10.1007/s00330-012-2621-0 (2013).
47. Brügger, M. et al. Tracing toothache intensity in the brain. *J. Dental Res.* **91**(2), 156–160. https://doi.org/10.1177/0022034511431253 (2012).
48. Brügger, M. et al. Taking sides with pain—lateralization aspects related to cerebral processing of dental pain. *Front. Hum. Neurosci.* **5**, 12. https://doi.org/10.3389/fnhum.2011.00012 (2011).
49. Rango, M. et al. Myoinositol content in the human brain is modified by transcranial direct current stimulation in a matter of minutes: a 1H-MRS study. *Magn. Reson. Med.* **60**(4), 782–789. https://doi.org/10.1002/mrm.21709 (2008).

50. Anwyl, R. Metabotropic glutamate receptor-dependent long-term potentiation. *Neuropharmacology* **56**(4), 735–740. https://doi.org/10.1016/j.neuropharm.2009.01.002 (2009).
51. Mangia, S. et al. Dynamics of lactate concentration and blood oxygen level-dependent effect in the human visual cortex during repeated identical stimuli. *J. Neurosci. Res.* **85**(15), 3340–3346. https://doi.org/10.1002/jnr.21371 (2007).
52. Magnotta, V. A. et al. Detecting activity-evoked pH changes in human brain. *Proc. Natl. Acad. Sci. USA* **109**(21), 8270–8273. https://doi.org/10.1073/pnas.1205902109 (2012).
53. Traynelis, S. F. & Chesler, M. Proton release as a modulator of presynaptic function. *Neuron* **32**(6), 960–962. https://doi.org/10.1016/S0896-6273(01)00549-9 (2001).
54. Wemmie, J. A., Price, M. P. & Welsh, M. J. Acid-sensing ion channels: advances, questions and therapeutic opportunities. *Trends Neurosci.* **29**(10), 578–586. https://doi.org/10.1016/j.tins.2006.06.014 (2006).
55. Wemmie, J. A., Zha, X. & Welsh, M. J. Acid-sensing ion channels (ASICs) and pH in synapse physiology. In *Structural and Functional Organization of the Synapse* (eds Hell, J. W. & Ehlers, M. D.) 661–681 (Springer, 2008).
56. Ziemann, A. E. et al. The amygdala is a chemosensor that detects carbon dioxide and acidosis to elicit fear behavior. *Cell* **139**(5), 1012–1021. https://doi.org/10.1016/j.cell.2009.10.029 (2009).
57. Uldry, M. et al. Identification of a mammalian H(+)-myo-inositol symporter expressed predominantly in the brain. *EMBO J.* **20**(16), 4467–4477. https://doi.org/10.1093/emboj/20.16.4467 (2001).
58. Kreis, R. Issues of spectral quality in clinical 1H-magnetic resonance spectroscopy and a gallery of artifacts. *NMR Biomed.* **17**(6), 361–381. https://doi.org/10.1002/nbm.891 (2004).
59. Henning, A. Proton and multinuclear magnetic resonance spectroscopy in the human brain at ultra-high field strength: A review. *NeuroImage* **168**, 181–198. https://doi.org/10.1016/j.neuroimage.2017.07.017 (2018).
60. Nassirpour, S., Chang, P., Avdievitch, N., Henning, A. Compressed sensing for high-resolution nonlipid suppressed 1 H FID MRSI of the human brain at 9.4T. *Magn. Reson. Med.* **80**(6), 2311–2325. https://doi.org/10.1002/mrm.27225 (2018).
61. Jia, Y. et al. Glutamate chemical exchange saturation transfer (GluCEST) magnetic resonance imaging in pre-clinical and clinical applications for encephalitis. *Front. Neurosci.* **14**, 750. https://doi.org/10.3389/fnins.2020.00750 (2020).
62. Haris, M., Cai, K., Singh, A., Hariharan, H. & Reddy, R. In vivo mapping of brain myo-inositol. *NeuroImage* **54**(3), 2079–2085. https://doi.org/10.1016/j.neuroimage.2010.10.017 (2011).

Acknowledgements

This study would not have been possible without the help of hypnosis experts Sandra Blabl, Chris Burch, Mike Schwarz, Claude Ribaux, and Hansruedi Wipf. We would also like to thank the volunteers who made themselves available free of charge for the experiments.

Author contributions

NM: Conceptualization, Formal analysis, Investigation, Methodology, Project administration, Supervision, Visualization, Writing—original draft, Writing—review and editing, Data curation, Funding acquisition, Resources, Software, Validation. PS: Investigation, Supervision, Writing—review and editing. Resources. NZ: Formal analysis, Software, Validation, review and editing. ES: Review and editing. MB: Conceptualization, Data curation, Formal analysis, Funding acquisition, Investigation, Methodology, Project administration, Resources, Software, Supervision, Validation, Visualization, Writing—original draft, Writing—review and editing.

Funding

The author(s) declare financial support was received for the research, authorship, and/or publication of this article. This study was funded by the University of Zurich and Hypnose.NET GmbH/OMNI Hypnosis International. This study received funding from Hypnose.NET GmbH/OMNI Hypnosis International. The funder was not involved in the study design, collection, analysis and interpretation of data, the writing of this article or the decision to submit it for publication. All authors declare no other competing interests.

Declarations

Competing interests

The authors declare no competing interests.

Additional information

Supplementary Information The online version contains supplementary material available at https://doi.org/10.1038/s41598-024-80795-3.

Correspondence and requests for materials should be addressed to M.B.